Below Level Central Pain Induced by Discrete Dorsal Spinal Cord Injury

Julie Wieseler,[1] Amanda L. Ellis,[1] Andrew McFadden,[1] Kimberley Brown,[1] Charlotte Starnes,[2] Steven F. Maier,[1] Linda R. Watkins,[1] and Scott Falci[2]

Abstract

Central neuropathic pain occurs with multiple sclerosis, stroke, and spinal cord injury (SCI). Models of SCI are commonly used to study central neuropathic pain and are excellent at modeling gross physiological changes. Our goal was to develop a rat model of central neuropathic pain by traumatizing a discrete region of the dorsal spinal cord, thereby avoiding issues including paralysis, urinary tract infection, and autotomy. To this end, dorsal root avulsion was pursued. The model was developed by first determining the number of avulsed dorsal roots sufficient to induce below-level hindpaw mechanical allodynia. This was optimally achieved by unilateral T13 and L1 avulsion, which resulted in tissue damage confined to Lissauer's tract, dorsal horn, and dorsal columns, at the site of avulsion, with no gross physical changes at other spinal levels. Behavior following avulsion was compared to that following rhizotomy of the T13 and L1 dorsal roots, a commonly used model of neuropathic pain. Avulsion induced below-level allodynia that was more robust and enduring than that seen after rhizotomy. This, plus the lack of direct spinal cord damage associated with rhizotomy, suggests that avulsion is not synonymous with rhizotomy, and that avulsion (but not rhizotomy) is a model of central neuropathic pain. The new model described here is the first to use discrete dorsal horn damage by dorsal root avulsion to create below-level bilateral central neuropathic pain.

Key words: avulsion; central pain; rhizotomy; spinal cord injury

Introduction

CENTRAL NEUROPATHIC PAIN is a frequent consequence of diverse neurological disorders, including multiple sclerosis, stroke, syringomyelia, traumatic brain injury, tumors, epilepsy, and spinal cord injury (SCI). Within the SCI population, chronic pain occurs in approximately 65% of patients, and within this group approximately 34% describe the pain as severe and intolerable (Baastrup and Finnerup, 2008; Siddall et al., 2003; Siddall, 2009). Patients experiencing this intense pain are often depressed and suicidal. The pain is not only debilitating, but for the most part it is intractable to treatment. Analysis of current pharmacotherapies for central neuropathic pain is limited due to the lack of randomized, controlled studies. The little information that is available indicates that the current pharmacological treatments are no more effective than has been reported for peripheral neuropathies, 50% pain relief in 1 out of 2–3 patients (Beniczky et al., 2005; McQuay et al., 1995, 1996).

Currently, animal models of central neuropathic pain induced by SCI rely on extensive trauma to the spinal cord (e.g., contusion or hemisection). These models are often chosen for study because they capture the diverse symptomatology characteristic of this clinical population. Here we describe a new model of central neuropathic pain created by a less disruptive lesion to the spinal cord. The unilateral lesion is created by rapid avulsion of dorsal roots from the spinal cord, thereby creating deafferentation as well as disruption of afferent projection regions (i.e., Lissauer's tract, the dorsal root entry zone, and the dorsal columns), while leaving the ventral and contralateral aspects intact. This discrete damage avoids urinary tract infection and paralysis, and at most induces delayed, transient autotomy in a minority of animals. This new model may allow changes specific to the development of centrally-mediated pain enhancement to be studied. It is expected that the data from this less traumatic model will complement and expand those from other models.

[1]Department of Psychology and Neuroscience and the Center for Neurosciences, University of Colorado at Boulder, Boulder, Colorado.
[2]Craig Hospital, Englewood, Colorado.

This new model was based in part on clinical reports of dorsal root avulsion from the spinal cord dorsal horn, such as that which occurs as a result of automobile and motorcycle accidents (Berman et al., 1998; Carlstedt, 2008). These motor vehicle accidents are the most common cause of spinal cord injuries, accounting for approximately 35% of new spinal cord injuries each year in the United States (DeVivo, 1997). Within this clinical population, assessment of neuronal activity at the avulsion site reveals spontaneous neuroelectrical hyperactivity (Edgar et al., 1993). Additionally, electrical hyperactivity in the dorsal horn after trauma to the thoracolumbar cord can cause below-level pain (Edgar et al., 1993; Falci et al., 2002), and such below-level pain with hyperactivity follows a specific somatotopic map (Falci et al., 2002). The new SCI model described here was developed guided by these data. With our model, the injury is limited to the dorsal horn of the avulsed roots in the thoracolumbar cord, and consistent with clinical data, the dorsal horn injury leads to below-level pain in the hindpaw.

The novel model of SCI-induced central neuropathic pain described here allows us to behaviorally evaluate the rats without compromising their health or motor function. To this end, our model utilizes unilateral avulsion of the T13 and L1 dorsal roots to induce bilateral central neuropathic pain below the dermatomal level of injury (hindpaw allodynia, or below-level pain). In our model the dura is retracted, the roots are avulsed, and the spinal cord is then covered with sterile saline–moistened surgical sponge, followed by suturing of the muscle and skin in layers. To demonstrate that dorsal root avulsion differs from simple T13 and L1 unilateral root transection (rhizotomy), we compared mechanical allodynia and spinal cord anatomical changes in response to these two procedures.

Methods

Subjects

Male Sprague-Dawley rats (350–400 g; Harlan Sprague-Dawley, Inc., Indianapolis, IN) were pair-housed with food and water available *ad libitum*. Room temperature was maintained at $24 \pm 1°C$ with a 12-h light:12-h dark cycle. The rats were allowed a minimum of 1 week to habituate to the colony room prior to surgery and testing. Following surgery the animals were singly housed. All protocols were approved by the University of Colorado Institutional Animal Care and Use Committee.

Surgery

Under isoflurane anesthesia, the appropriate spinal levels were identified using landmarks relative to the vertebral thoracic (T) 13 floating rib, and a dorsal laminectomy was performed. The exposed dura was then reflected. The dorsal roots were identified and gently isolated. For the rhizotomy procedure, each root was transected with microscissors approximately 2–3 mm distal from the dorsal root entry zone, keeping tension between the root and spinal cord to a minimum in order to avoid dorsal horn damage. For the avulsion procedure, each root was firmly grasped with microforceps at the dorsal root entry zone and rapidly torn away from the dorsal horn, and then transected to remove the cut ends of the dorsal roots away from the damaged dorsal horn (Fig. 1).

Methods development included studies to identify the minimal combination of avulsed dorsal roots that create robust below-level mechanical allodynia as measured in the hindpaws (L4–L6). To this end, we bilaterally compared the behavioral consequences of the following surgical manipulations: unilateral T13 + L1 avulsion versus unilateral T12 + T13 + L1 avulsion versus sham; unilateral T13 + L1 avulsion versus unilateral T13 avulsion versus unilateral L1 avulsion versus sham; and lastly, unilateral T13 + L1 avulsion versus bilateral T13 + L1 avulsion versus sham. Sterile saline-moistened surgical sponge was placed over the exposed spinal cord, the muscle was sutured in layers with sterile 3-0 silk, and the skin was closed with stainless steel wound clips. Upon completion of surgery, the rats were individually placed in their home cages, with foam padding added for a few hours to protect the rats from inadvertent SCI during the brief ataxic period associated with recovery from anesthesia, during which all animals tend to walk awkwardly, falling against the sides of the cage or rolling, thus putting them at risk for bruising the spinal cord segment newly exposed by laminectomy. Sham-operated rats were treated identically, undergoing laminectomy and opening of the dura, but without nerve avulsion or transection. Antibiotics were administered to all rats at the time of surgery and then daily for 4 days.

Behavioral assessments

Hindpaw mechanical allodynia. Absolute thresholds were determined in the sciatic innervation area of both ipsilateral and contralateral hindpaws, using the up-down method with a series of calibrated filaments (von Frey test), as previously described in detail elsewhere (Milligan et al.,

FIG. 1. Photograph of spinal cord immediately after dorsal root avulsion. Following laminectomy and retraction of the dura, the dorsal roots are isolated and rapidly avulsed from the spinal cord. This avulsion disrupts the physical integrity of the spinal cord, leaving holes at the point of dorsal root entry.

2001). All testing was performed blinded with respect to group assignment. Briefly, a logarithmic series of 10 calibrated Semmes-Weinstein monofilaments (von Frey hairs; Stoelting, Wood Dale, IL) were applied to both the left and right hindpaws in random order to determine the stimulus intensity threshold stiffness required to elicit a paw withdrawal response. Log stiffness of the hairs is determined by $\log_{10}$ (milligrams$\times$10). The 10 stimuli had the following log-stiffness values: 3.61 (0.407 g), 3.84 (0.692 g), 4.08 (1.202 g), 4.17 (1.479 g), 4.31 (2.041 g), 4.56 (3.630 g), 4.74 (5.495 g), 4.93 (8.511 g), 5.07 (11.749 g), and 5.18 (15.136 g). This range of monofilaments produces a logarithmically-graded slope when interpolating a 50% response threshold of stimulus intensity (expressed as $\log_{10}$ [milligrams$\times$10]). Assessments were made before (baseline), and at specific times after avulsion or rhizotomy, as detailed below. The behavioral responses were used to calculate the 50% paw withdrawal threshold (absolute threshold), by fitting a gaussian integral psychometric function by using a maximum-likelihood fitting method. This fitting method allows parametric statistical analyses (Harvey, 1986).

Thermal hyperalgesia. Latencies for the behavioral response to radiant heat stimuli applied to each hindpaw were assessed using the Hargreaves test (Hargreaves et al., 1988), as previously described in detail elsewhere (Milligan et al., 2000). All testing was performed blinded with respect to group assignment. Briefly, paw withdrawal values for both the left and right hindpaws were separately calculated from an average of three consecutive withdrawal latencies of each paw measured at 15-min intervals. Voltage to the heat source was adjusted to yield baseline latencies ranging from 8–11 sec, and a cut-off time of 20 sec was imposed to avoid tissue damage. Assessments were made before (baseline) and at specific times after surgery, as detailed below. The order of paw testing varied randomly.

Grid-walk test. In order to quantify deficits in motor control, the rats were trained to walk across a 67-cm-long horizontal ladder with round metal bars (0.6 cm diameter), spaced 2.54 cm apart. During all baseline and postoperative testing, the animals were required to walk across the ladder three consecutive times without stopping. In order to complete the task successfully, the animals had to step rhythmically and use fine control of posture and locomotion. This required optimal integration of both the sensory and descending motor pathways. The rats underwent three separate habituation periods the week prior to surgery to acclimate to the novelty of the horizontal ladder. The day before surgery the rats underwent testing for baseline measures. The animals were tested once a week beginning 14 days post-surgery. The total time it took to cross the ladder and the total number of hindlimb footfalls (errors) was recorded for each trial. The number of errors from each trial was then averaged to get a mean error rate for every animal.

Preparation and processing of tissue for anatomy

The rats were overdosed with sodium pentobarbital, and then transcardially perfused with 0.9% saline. After dissection, the spinal cord was transferred to a 15-mL tube containing 4% paraformaldehyde in 0.1 M phosphate buffer (PB).

After fixation at 4°C overnight, the spinal cords were transferred to 15-mL tubes containing 30% sucrose in 0.1 M PB and cryoprotected at 4°C for a minimum of 24 h. The spinal cords were transversely blocked into two 5-mm sections, one section including the site of injury, and another 10 mm caudal to the site of injury. This latter site corresponds to spinal level lumbar (L)5-L6, the spinal site from which responses to mechanical and thermal stimuli were elicited. These tissues were sectioned at 60 μm in a cryostat and thaw mounted on gelatin-coated slides. All sections were serially mounted so that the extent of damage could be determined.

To examine whether rhizotomy or avulsion differentially disrupted the anatomical structure of the dorsal horn, T13-L1 and L5-L6 slices were compared from rhizotomy, avulsion, or sham-operated rats, and processed in two ways. For one, we took advantage of the interaction between 3′,3-diaminobenzidine (DAB; Sigma-Aldrich, St. Louis, MO), and endogenous peroxidases expressed by red blood cells. The spinal cord slices were reacted using DAB for 15 min. Glucose oxidase (type V-s, 0.02%; Sigma-Aldrich), and β-D-glucose (0.1%) were used to generate hydrogen peroxide. Nickelous ammonium sulfate was added to the DAB solution (0.025% w/v) to intensify the reaction product. The slides were dried overnight, cleared, and cover-slipped with slide-mounting fluid. Another set of slides was stained with cresyl violet to show the physical disruption of the tissue. A subset of the DAB-stained slides also underwent cresyl violet counterstaining; however, due to the darkness of the DAB staining, the cresyl violet counterstaining of these tissues was difficult to visualize.

Statistical analysis

All data were analyzed by analysis of variance (ANOVA) using GraphPad Prism version 5.00 for Mac OS X (GraphPad Software, San Diego, CA). Ipsilateral and contralateral behavioral data were analyzed individually. In the initial experiments to determine the optimal dorsal root combination to avulse, group differences were analyzed by comparing area under the curve (AUC), as previously described by Jones and Sorkin (Jones and Sorkin, 2004). AUC values were calculated from absolute threshold values, from 0 up to the threshold response of each animal across time. Decreased AUC reflects an increase in mechanical allodynia.

Results

Comparison of the number and laterality of avulsed dorsal root combinations on below-level hindpaw mechanical allodynia

The testing area on the hindpaw is innervated primarily by sciatic nerve axons from L4–L6 dorsal root ganglia (Takahashi and Nakajima, 1996). Thus afferent information arising from the hindpaw enters the spinal cord $\sim$ 4 spinal segments below the avulsion injury. This is important, as below-level pain is generally defined as pain greater than two dermatomal levels below the site of injury (Siddall and Finnerup, 2006). Our goal was to avulse as few dorsal roots as possible that would result in profound and long-lasting hindpaw mechanical allodynia. Studies were used to identify the optimal number and laterality of roots avulsed for creating robust hindpaw allodynia with minimal neurotrauma (Figs. 2, 3, and 4). Here we tested both ipsilateral and contralateral hindpaw mechanical
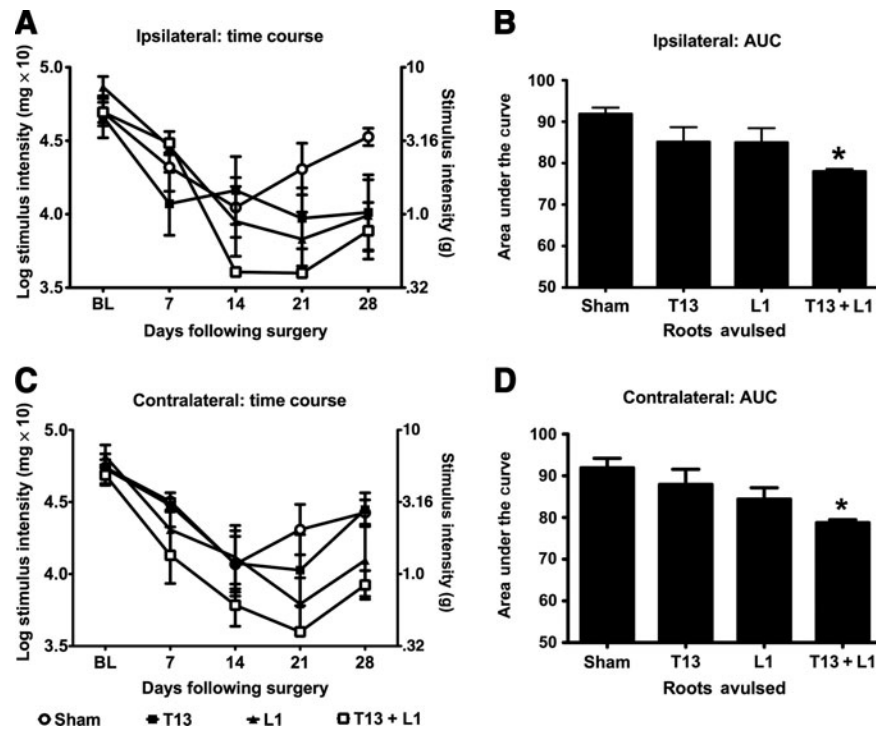
FIG. 2. T13 + L1 unilateral dorsal root avulsion leads to more robust hindpaw mechanical allodynia than unilateral avulsion of the T13 or L1 dorsal roots alone. The first step in developing the avulsion model was to determine the minimum number of roots to avulse that would lead to hindpaw mechanical allodynia. To this end, the individual unilateral roots T13 and L1 were avulsed, as were combined unilateral T13 + L1. The data are presented in two ways: as line graphs representing the time course of the ipsilateral (**A**) and contralateral (**C**) allodynia, and as bar graphs showing the AUC, on which statistical analyses were performed (ipsilateral **B**, and contralateral **D**). Avulsion of either the T13 or the L1 dorsal root alone resulted in a less robust mechanical allodynia than did the combined avulsion of T13 + L1, both ipsilateral and contralateral to the avulsion ($n = 4-5$ per group; *$p < 0.05$ compared to sham animals; AUC, area under the curve).

allodynia. For each of these studies, a one-way ANOVA was conducted on the area under the curve (AUC; described above).

As a first step, we compared the efficacy of either unilateral avulsion of a single dorsal root (T13 or L1), and unilateral avulsion of the T13 + L1 dorsal roots for producing below-level hindpaw mechanical allodynia, both ipsilateral and contralateral to injury. As shown in Figure 2, single-root avulsion did not result in as robust an allodynic response, ipsilaterally or contralaterally, as did the combined avulsion of T13 + L1. The one-way ANOVA comparing ipsilateral AUC of sham, T13 alone, L1 alone, and T13 + L1 avulsion was significant [$F(3,18) = 3.946$, $p = 0.03$; Fig. 2B], as was the comparison of these groups on the contralateral side [$F(3,17) = 3.715$, $p = 0.03$; Fig. 2D]. *Post-hoc* analysis of the AUCs revealed that the T13 + L1 avulsion group was significantly more allodynic than sham animals ($p < 0.05$). In contrast, neither the T13 or L1 avulsion groups differed from sham animals. These data point to the combined avulsion of T13 + L1 as being the more robust option.

The next step was to test whether unilateral avulsion of three dorsal roots, T12 + T13 + L1, would significantly enhance mechanical allodynia compared to T13 + L1 avulsion. T12 was chosen as the third dorsal root to be avulsed, rather than L2, in order to keep the caudal-most avulsion level constant between groups. As shown in Figure 3, comparable ipsilateral and contralateral below-level allodynia was

induced across time by both avulsion procedures. AUC analysis supported that both of these avulsions reliably lowered mechanical response thresholds compared to shams, ipsilaterally [$F(2,10) = 8.620$, $p = 0.01$; Fig. 3B], and contralaterally [$F(2,10) = 6.938$, $p = 0.02$; Fig. 3D]. *Post-hoc* analyses of ipsilateral and contralateral data indicated that in both cases unilateral T13 + L1 and unilateral T12 + T13 + L1 avulsion groups did not significantly differ from each other; however, both exhibited significantly lower response thresholds compared to sham-operated controls ($p < 0.05$). Thus, given the goal of minimizing trauma, T13 + L1 avulsion was selected for further study.

Lastly, we tested if bilateral T13 + L1 avulsion resulted in reliably greater hindpaw allodynia than unilateral T13 + L1 avulsion. Figure 4 shows that unilateral and bilateral avulsion of T13 + L1 equally induce ipsilateral and contralateral hindpaw mechanical allodynia. The one-way ANOVA comparing the AUC for sham, unilateral T13 + L1 avulsion, and bilateral T13 + L1 avulsion was significant for both hindpaws, ipsilaterally [$F(2,11) = 7.719$, $p = 0.01$; Fig. 4B], and contralaterally [$F(2,10) = 8.663$, $p = 0.01$; Fig. 4D]. *Post-hoc* analyses showed that the ipsilateral and contralateral AUC for both bilateral T13 + L1 avulsion and unilateral T13 + L1 avulsion were significantly lower compared to the sham group ($p < 0.05$); however, they were not statistically significantly different from each other. That is, unilateral T13 + L1 and bilateral T13 + L1 avulsion induced ipsilateral and contralateral
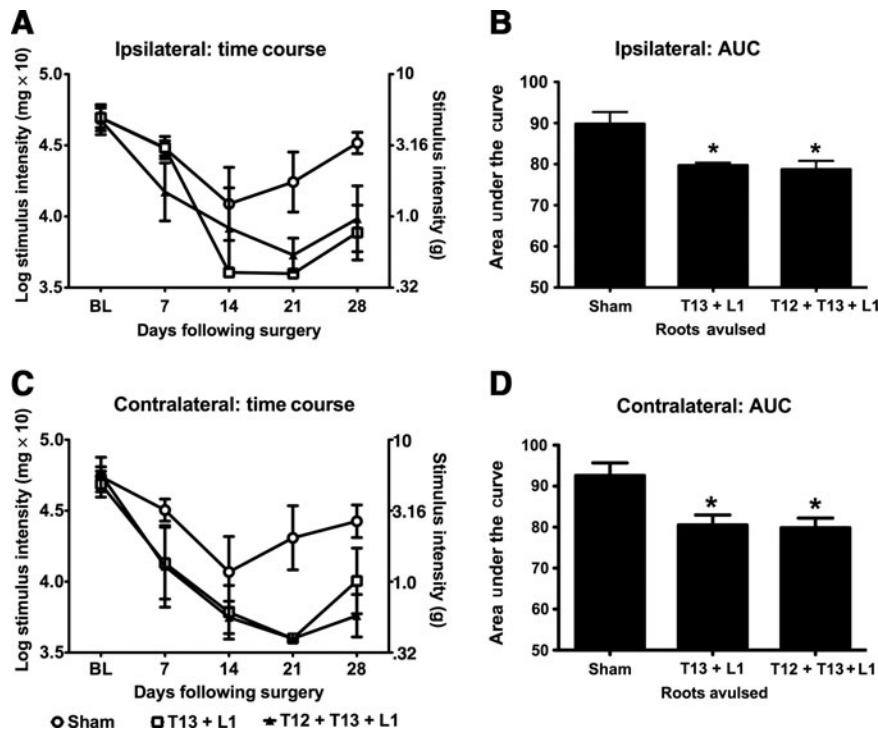
FIG. 3. T13 + L1 unilateral dorsal root avulsion results in robust hindpaw allodynia comparable to that induced by unilateral avulsion of T12 + T13 + L1. After identifying that unilateral avulsion of two dorsal roots induced more robust allodynia than single-root avulsion, we tested whether avulsion of three dorsal roots would be more robust than two. Unilateral avulsion of T13 + L1 induction of behavior was compared to that of unilateral avulsion of T12 + T13 + L1. Ipsilateral (**A** and **B**) and contralateral (**C** and **D**) time course data are presented, as are the AUC data, which were statistically analyzed. Unilateral avulsion of three dorsal roots (T12, T13, and L1) did not result in greater hindpaw mechanical allodynia than unilateral avulsion of two dorsal roots (T13 and L1; $n = 3–4$ per group; $*p < 0.05$ compared to sham animals; AUC, area under the curve).

hindpaw allodynia equally well, and statistically significantly greater than sham operation. Taken together with the data above, the optimal model for creating robust below-level allodynia with minimal spinal trauma was determined to be unilateral T13 + L1 dorsal root avulsion. A significant additional advantage of choosing unilateral over bilateral avulsion is the ability to easily study the induction of below-level pain induced contralaterally as well as ipsilaterally relative to the injury site. Bilateral avulsion obscures the detection and interpretation of contralateral versus ipsilateral pain modulation. Thus unilateral T13 + L1 dorsal root avulsion was used for the remainder of the studies.

Unilateral avulsion of the T13 and L1 dorsal roots leads to sustained bilateral hindpaw allodynia, but not thermal hyperalgesia

The next experiment expanded on the initial studies and tested the length of time that unilateral T13 + L1 avulsion induced bilateral hindpaw mechanical allodynia. Unilateral avulsion of T13 + L1 leads to below-level ipsilateral and contralateral mechanical allodynia in the hindpaws compared to sham animals (Fig. 5A and B), but not thermal hyperalgesia (data not shown). The repeated-measures ANOVA interaction between surgery and time comparing mean radiant heat paw withdrawal latencies was not significant for the ipsilateral hindpaw [$F_{(8,48)} = 0.30$, $p = 0.96$], or the contralateral hindpaw [$F_{(8,48)} = 0.56$, $p = 0.84$]. The corresponding main

effects also did not reach significance, ipsilaterally [surgery: $F_{(1,36)} = 0$, $p = 0.98$; time: $F_{(6,36)} = 22.85$, $p = 0.06$], and contralaterally [surgery: $F_{(1,36)} = 0$, $p = 0.96$; time: $F_{(6,36)} = 15.06$, $p = 0.32$]. In contrast, the repeated-measures ANOVA interaction between surgery and time for ipsilateral hindpaw allodynia was significant [$F_{(10,100)} = 12.41$, $p < 0.001$]. The unilateral avulsion of the T13 + L1 group showed statistically significantly greater ipsilateral hindpaw allodynia than the sham group, beginning at day 21, and these two groups remained statistically significantly different through day 63 ($p < 0.05$). There were main effects in the two-way ANOVA for surgery and time [$F_{(1,100)} = 11.52$, $p < 0.005$, and $F_{(10,100)} = 7.16$, $p < 0.001$, respectively], but no reliable interaction was seen between surgery and time for contralateral hindpaw allodynia ($p = 0.09$). This avulsion group showed statistically significantly greater hindpaw allodynia than the sham-operated group in the contralateral (mirror-image) paw compared to sham animals on days 21 and 28 ($p < 0.05$).

Hindpaw mechanical allodynia following dorsal root avulsion is different from that induced by rhizotomy

The unilateral T13 + L1 avulsion group showed statistically significantly more enduring and robust ipsilateral and contralateral hindpaw mechanical allodynia compared to the unilateral T13 + L1 rhizotomy group and the sham-operated group (Fig. 6). The two-way ANOVA interaction between surgery and time was significant for the ipsilateral hindpaw
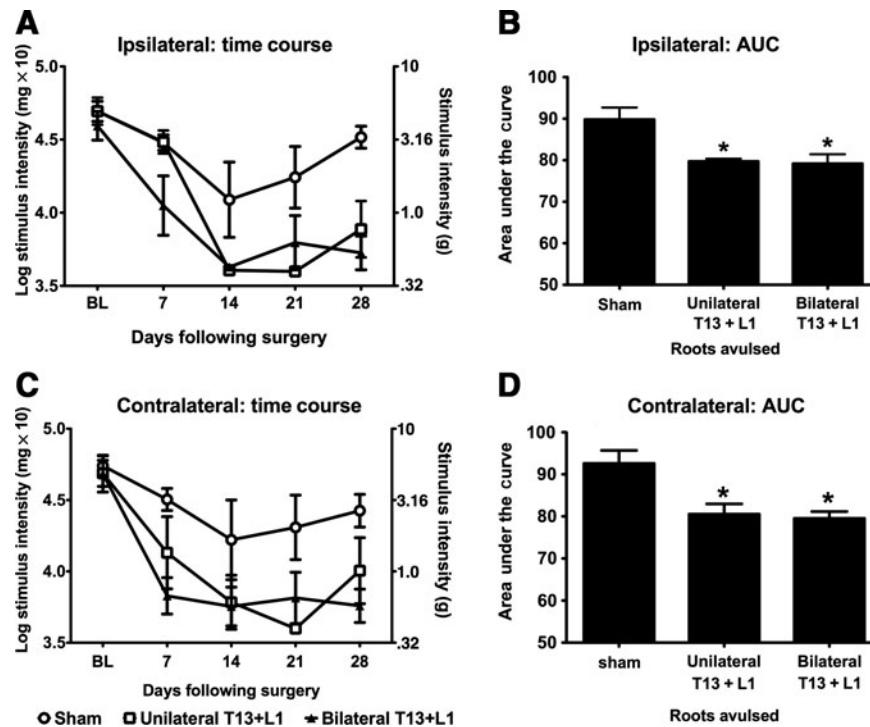
FIG. 4. T13 + L1 unilateral dorsal root avulsion results in robust hindpaw mechanical allodynia consistent with that created by T13 + L1 bilateral dorsal root avulsion. Unilateral avulsion was compared to bilateral avulsion to determine if bilateral avulsion of T13 + L1 would lead to more robust hindpaw allodynia than unilateral avulsion alone. Ipsilateral (**A** and **B**) and contralateral (**C** and **D**) time-course data are presented, as are the AUC data, which were statistically analyzed. Bilateral avulsion did not induce greater hindpaw mechanical allodynia than unilateral avulsion ($n = 4$ per group; *$p < 0.05$ compared to sham animals; AUC, area under the curve).

[$F(16,168) = 5.316$, $p < 0.0001$]. Unilateral T13 + L1 avulsion induced greater ipsilateral hindpaw allodynia than unilateral T13 + L1 rhizotomy and sham-operated rats ($p < 0.05$). The two-way ANOVA interaction between surgery and time for the contralateral hindpaw was also significant [$F(16,168) = 4.574$, $p < 0.0001$]. Similarly, unilateral T13 + L1 avulsion resulted in greater hindpaw mechanical allodynia on the contralateral (mirror-image) side compared to rhizotomy and sham operated rats ($p < 0.05$).

Dorsal root avulsion causes tissue disruption and injury to the dorsal spinal cord

Visualization of the avulsion injury by staining with DAB and its reaction with red blood cells (Fig. 7), or via cresyl violet staining (Fig. 8), revealed clear macroscopic differences between the dorsal spinal cords following avulsion versus rhizotomy surgery. In the method described here, root avulsion rips the dorsal root from the dorsal root entry zone of the spinal cord, and as such physically disrupts the fine structure of the superficial layers of the dorsal horn, as is made apparent by the cresyl violet stain, and also causes an influx of red blood cells representative of hemorrhage and dorsal horn trauma. This physical disruption demonstrated by the cresyl violet stain and corresponding red blood cell accumulation spans laminae I, II, and III, and to a lesser degree lamina IV. As shown here, the white matter did not appear to be physically disrupted. While no apparent physical disruption was seen in the dorsal spinal columns with the cresyl violet stain, the influx of red blood cells showed some cells outside of the

dorsal horn, in Lissauer's tract and the dorsal columns. In contrast, rhizotomy surgery did not result in physical disruption of the dorsal spinal cord or in red blood cell influx. Thus the avulsion method described here results in an injured spinal cord dorsal horn.

Dorsal root avulsion produces at most only mild and transient effects on motor and autotomy scores, and no urinary tract infections

Motor changes were assessed using grid-walk behavior on a horizontal ladder. Initially following surgery, both unilateral T13 + L1 dorsal root avulsion and sham-operated rats misstepped equally when walking across the horizontal ladder, with the number of missteps ranging from 1 to 2 missteps per trial (Fig. 9). This is lower than the numbers seen following dorsal column lesions (Davies et al., 2006), or spinal cord contusion (McEwen and Springer, 2006), both which were been reported to average 7 missteps. During the first 14 days, even though the number of missteps did not differ between groups, subtle differences were observed. During this period of time the avulsion-operated rats, while appearing to completely put their weight on both hindpaws, demonstrated awkward movements of the ipsilateral hindpaw. This initial mild motor impairment resolved within 14 days, at which point blinded observers could not discern which rats had had avulsion versus sham surgery. While not systematically quantitified, the impression was that the behavioral profile observed would be comparable to a rating of 19–20 on the Basso, Beattie, and Bresnahan rank scores
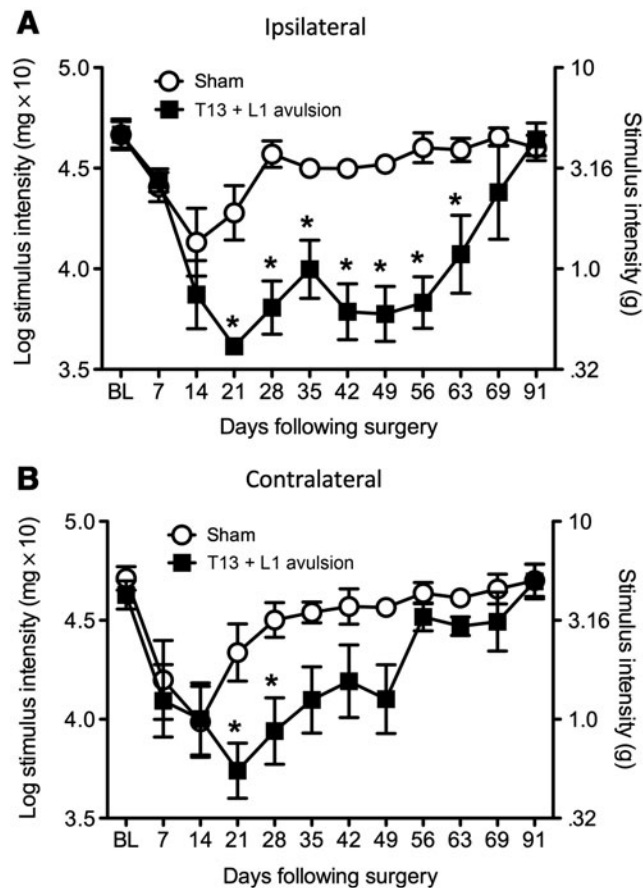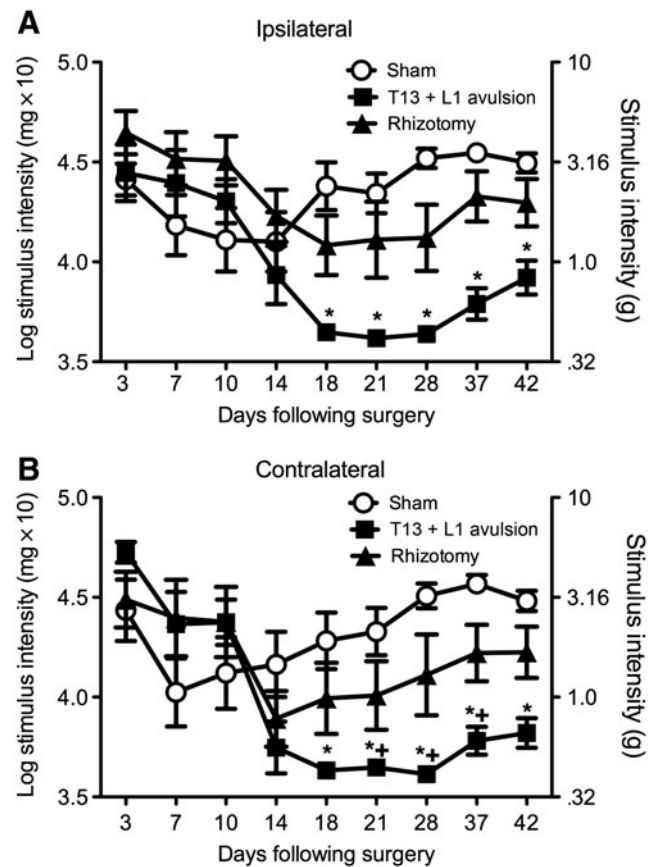
FIG. 5. Unilateral dorsal root avulsion leads to bilateral below-level mechanical allodynia. Following baseline assessment of the response to calibrated von Frey filaments, the rats underwent avulsion surgery. Avulsion of T13 + L1 induced ipsilateral and contralateral hindpaw mechanical allodynia that became robust within 21 days post-surgery ($n = 6$ per group; **A**, ipsilateral; **B**, contralateral; *$p < 0.05$ compared to sham animals; BL, baseline).

FIG. 6. Avulsion of T13 + L1 dorsal roots creates a more robust mechanical allodynia profile than rhizotomy of the same roots. Following baseline assessment of the response to calibrated von Frey filaments, the rats underwent avulsion surgery or rhizotomy surgery. Avulsion of the T13 + L1 dorsal roots induced more robust below-level bilateral mechanical allodynia than did rhizotomy ($n = 8$ per group; **A**, ipsilateral; **B**, contralateral; *$p < 0.05$ compared to sham animals; $+ p < 0.05$ compared to rhizotomy).

during the first 14 days, and after that to a rating of 21 (Basso et al., 1995).

Additionally, following avulsion none of the rats developed urinary tract infections or paralysis. Both sham- and avulsion-operated rats showed transient paresis in the hind legs that generally resolved within 14–21 days. A small number of rats (approximately 4%) did develop mild autotomy between 21 and 28 days post-surgery, most often located just above the knee, which was treated with topical antibiotics and resolved in approximately 7 days. The behavioral profiles of these animals did not differ from those that did not develop autotomy.

Discussion

The present series of studies demonstrate that unilateral low thoracic plus upper lumbar dorsal root avulsion causes discrete damage to the dorsal horn at the avulsion site, as well as persistent below-level bilateral mechanical allodynia measurable in the hindpaws. Importantly, behavioral measurement of below-level hindpaw mechanical allodynia is not confounded by paralysis or infection secondary to urinary

retention. While the spinal cord is minimally damaged, the rat is otherwise healthy and without the complications generally associated with commonly used models of SCI. This is the first model to use unilateral T13−L1 dorsal root avulsion to induce below-level mechanical allodynia in the hindpaws, and to model chronic central pain. Notably, the mechanical allodynia slowly develops over time, reliably within the first 14 days, with some animals developing allodynia more rapidly than others. This pattern of mechanical allodynia development is consistent with clinical reports of below-level pain, as central neuropathic pain does not develop immediately, but rather slowly develops over 0.5−30 months following injury (Baastrup and Finnerup, 2008). Following surgery, both avulsion and sham-operated rats did show reductions in the mechanical threshold over the first 14 days, which was not surprising given the tissue trauma inherent to the sham surgery as well. However, in contrast to the resolving allodynia observed in the sham groups after this time, allodynia continued to develop in rats with avulsion. For these rats, allodynia was maintained until approximately 9 weeks after surgery. As the mechanisms underlying acute and chronic pain differ, the long-lasting allodynic state induced by
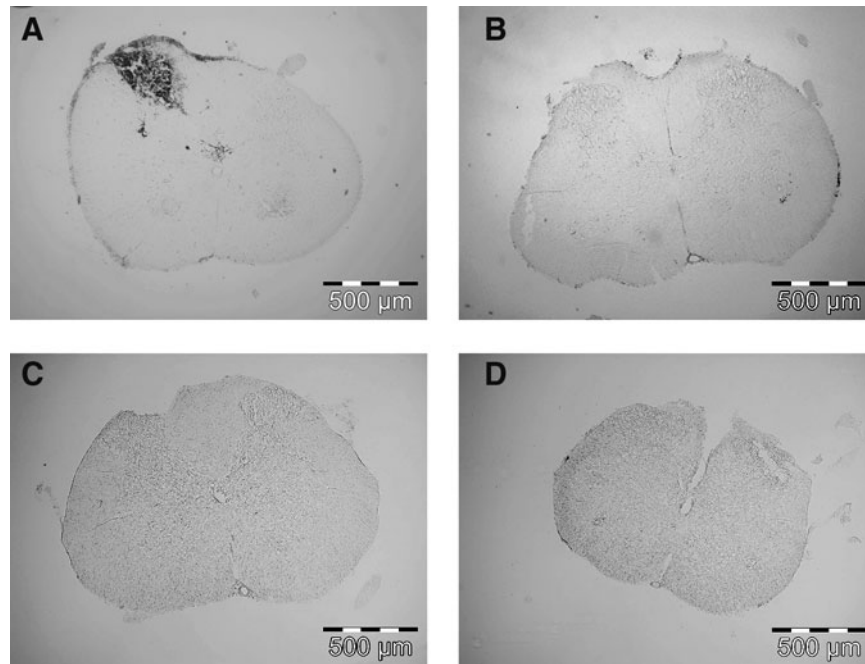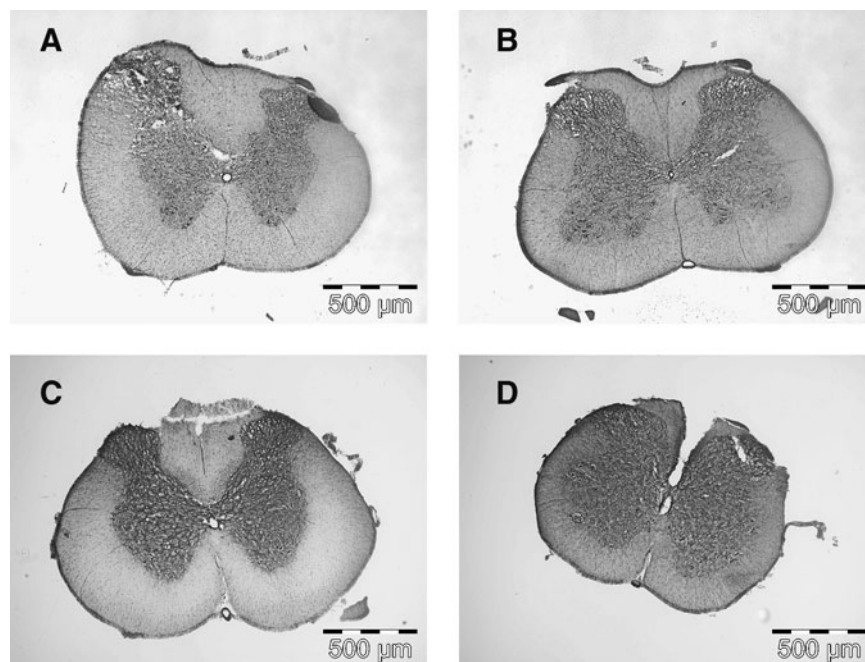
FIG. 7. Avulsion of dorsal roots dramatically disrupted the dorsal spinal cord, causing an influx of blood cells only at the lesion site, while rhizotomy did not result in blood cell influx. Incubation of tissue with 3′,3-diaminobenzidine (DAB) revealed an influx of blood cells into the site of avulsion, but not at the spinal site of the below-level pain (**A**, T13−L1; **B**, L4−L6). No influx of blood was found at either site following rhizotomy (**C**, T13−L1; **D**, L4−L6).

unilateral T13 + L1 avulsion indicates that this model will prove useful for drug testing aimed at understanding and treating SCI pain of prolonged duration.

Pain that arises in the corresponding body part contralateral to the injured site is referred to as mirror-image pain. Here

we show that unilateral dorsal root avulsion resulted not only in ipsilateral below-level pain, but also contralateral below-level pain. The pain on the contralateral side may be caused by similar mechanisms to those underlying mirror-image pain observed following peripheral neuropathy (Huang and Yu,

FIG. 8. Avulsion of dorsal roots physically disrupted the dorsal horn. Rhizotomy did not physically alter the dorsal spinal cord. Staining tissues with cresyl violet revealed the physical disruption at the site of avulsion, but not at the spinal site of below-level pain (**A**, T13−L1; **B**, L4−L6). The tissue was not disrupted following rhizotomy (**C**, T13−L1; **D**, L4−L6).
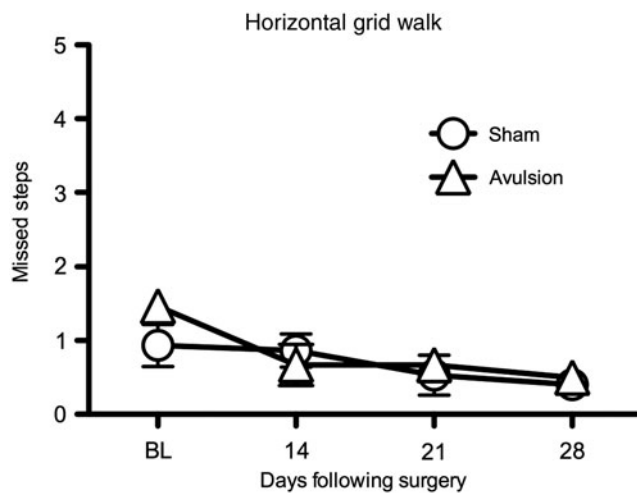
FIG. 9. Avulsion of dorsal roots did not alter horizontal grid-walk performance. Motor function was assessed using the grid walk, in which the rats were trained to rapidly cross a horizontal ladder, and baseline measures were taken prior to surgery. No differences were observed between the sham group and the avulsion group ($n = 5$ per group).

2010; Milligan et al., 2003; Spataro et al., 2004). The unilateral damage confined to the dorsal spinal cord makes the avulsion model appealing for further studying this mirror-image-like pain in central neuropathy.

Studies of recovery of motor function have extensively used ventral root avulsion as a model of SCI (Chu et al., 2009; Penas et al., 2009; Rodrigues Hell et al., 2009; Scorisa et al., 2009; Su et al., 2009; Zhou et al., 2008), with to our knowledge only one prior article considering root avulsion and allodynia (Bigbee et al., 2007). In that paper, Bigbee and associates avulsed L6−S1 ventral roots from the spinal cord and measured at-level (the L5 dermatome level) mechanical allodynia and thermal hyperalgesia in the hindpaw. Similarly to the below-level findings presented here, avulsion induced at-level hindpaw mechanical allodynia within 2 weeks post-surgery, that continued through week 7, without affecting thermal response thresholds. Other models of SCI, including spinal transverse hemisection at spinal level T13 (Gwak and Hulsebosch, 2009; Gwak et al., 2004; Hains et al., 2003), contusion injury at spinal level T8 or T10 (Hulsebosch et al., 2000; Lampert et al., 2006; Tan et al., 2008; Vierck et al., 2000; Zhao et al., 2007), and chemical lesioning with quisqualic acid (Abraham et al., 2001a, 2001b; Gorman et al., 2001; Yezierski et al., 1998), have all been reported to result in long-lasting bilateral below-level mechanical allodynia, as well as bilateral below-level thermal hyperalgesia. While the pattern of allodynia but no hyperalgesia has been seen following peripheral nerve inflammation (Chacur et al., 2001; Milligan et al., 2003; Sorkin et al., 2002; Thompson et al., 1996), allodynia without hyperalgesia following central trauma has only been previously reported by Bigbee and colleagues, with L6−S1 ventral root avulsion (Bigbee et al., 2007). The degree of trauma and the corresponding immune response has been proposed to explain this response pattern when it is seen following peripheral nerve injury (Sorkin et al., 2002; Thompson et al., 1996). When grooming behavior was used as a measure of neuropathic pain (Abraham et al., 2001a, 2001b; Yezierski,

2006), the onset and severity of grooming, and the expression of thermal hyperalgesia, were dependent on the degree of gray-matter tissue damage caudal and rostral to the initial injury. Given the very mild degree of injury induced by avulsing nerve roots from the spinal cord, it seems likely that these factors may also explain why mechanical allodynia, but not thermal hyperalgesia, were observed here, in contrast with other more traumatic spinal injury models that induce both phenomena below the level of injury.

In reviewing the literature, the term "avulsion" has often been equated with rhizotomy and deafferentation. Deafferentation is a general term referring to the disruption of afferent nerve communication. As such, both avulsion of dorsal roots from the spinal cord and rhizotomy are different means of deafferentation. While avulsing dorsal roots does cause deafferentation, it is not the equivalent of severing the rootlets external to the spinal cord (Ovelmen-Levitt et al., 1984). We considered here whether (1) the spinal cord anatomy is differentially affected by dorsal root avulsion versus rhizotomy, and (2) simply severing the connection from the dorsal root ganglia to the spinal cord was sufficient to induce the same behavioral profile and anatomical profile we observed following dorsal root avulsion from the spinal cord. Our spinal cord images (Figs. 7 and 8) show that while avulsion dramatically disrupts the spinal cord dorsal horn structure, rhizotomy does not. Future studies will characterize the microscopic changes (e.g., central arborization degeneration and neuronal state) that occur in the spinal cord over time. Below-level bilateral hindpaw mechanical allodynia was observed following both surgeries; however, the allodynia seen following avulsion was more robust and longer-lasting than that seen following rhizotomy. That is, greater mechanical allodynia resulted when deafferentation was accompanied by damage to the dorsal horn. Traumatizing the dorsal spinal cord gray matter induced below-level mechanical allodynia, and a mechanical-allodynia profile different from that of rhizotomy. Taken together, these data show that this unilateral T13−L1 avulsion model of central neuropathic pain differs significantly from rhizotomy, and thus suggests that the term "avulsion" be reserved for situations that include dorsal horn damage rather than simple deafferentation. This would be in keeping with the formal dictionary definition of avulsion as "the forcible tearing away of a body part by trauma or surgery".

Our model differs significantly from other models in that most aim to model the entire impact of SCI, and then to consider individual co-morbidities. Our model was developed to specifically study hindpaw mechanical allodynia, and as such our goal was to injure the spinal cord just enough to induce below-level allodynia. In doing so, discrete regions of the spinal cord were damaged, while leaving the ventral and contralateral aspects intact. As such, we have designed a unique, clinically relevant model of central neuropathic pain. As noted, we saw mild paresis in our animals, and importantly, equally in sham-operated controls, that generally resolved within 3 weeks following surgery, and we saw autotomy in a small number of animals, but neither issue interfered with hindpaw testing. Our future studies will thoroughly characterize the changes seen at different levels of the spinal cord, including neuronal damage and glial activity.

A significant challenge in the SCI field is translating findings from animal models to the clinical population. Much of

this is attributed to the inherent variability of clinical SCI. One way to gain more applicable information from animal models may be to develop models of specific aspects of the clinical symptomatology. Here the focus is on the exaggerated pain associated with SCI. Our hope is that this new model, combined with what has been learned using other models, will lead to a more successful translation from bench to bedside.

Acknowledgments

Author Disclosure Statement

No conflicting financial interests exist.

References

Abraham, K.E., McGinty, J.F., and Brewer, K.L. (2001a). Spinal and supraspinal changes in opioid mRNA expression are related to the onset of pain behaviors following excitotoxic spinal cord injury. Pain 90, 181–190.

Abraham, K.E., McGinty, J.F., and Brewer, K.L. (2001b). The role of kainic acid/AMPA and metabotropic glutamate receptors in the regulation of opioid mRNA expression and the onset of pain-related behavior following excitotoxic spinal cord injury. Neuroscience 104, 863–874.

Baastrup, C., and Finnerup, N.B. (2008). Pharmacological management of neuropathic pain following spinal cord injury. CNS Drugs 22, 455–475.

Basso, D.M., Beattie, M.S., and Bresnahan, J.C. (1995). A sensitive and reliable locomotor rating scale for open field testing in rats. J. Neurotrauma 12, 1–21.

Beniczky, S., Tajti, J., Timea Varga, E., and Vecsei, L. (2005). Evidence-based pharmacological treatment of neuropathic pain syndromes. J. Neural Transm. 112, 735–749.

Berman, J.S., Birch, R., and Anand, P. (1998). Pain following human brachial plexus injury with spinal cord root avulsion and the effect of surgery. Pain 75, 199–207.

Bigbee, A.J., Hoang, T.X., and Havton, L.A. (2007). At-level neuropathic pain is induced by lumbosacral ventral root avulsion injury and ameliorated by root reimplantation into the spinal cord. Exp. Neurol. 204, 273–282.

Carlstedt, T. (2008). Root repair review: basic science background and clinical outcome. Restor. Neurol. Neurosci. 26, 225–241.

Chacur, M., Milligan, E.D., Gazda, L.S., Armstrong, C., Wang, H., Tracey, K.J., Maier, S.F., and Watkins, L.R. (2001). A new model of sciatic inflammatory neuritis (SIN): induction of unilateral and bilateral mechanical allodynia following acute unilateral peri-sciatic immune activation in rats. Pain 94, 231–244.

Chu, T.H., Li, S.Y., Guo, A., Wong, W.M., Yuan, Q., and Wu, W. (2009). Implantation of neurotrophic factor-treated sensory nerve graft enhances survival and axonal regeneration of motoneurons after spinal root avulsion. J. Neuropathol. Exp. Neurol. 68, 94–101.

Davies, J.E., Huang, C., Proschel, C., Noble, M., Mayer-Proschel, M., and Davies, S.J. (2006). Astrocytes derived from glial-restricted precursors promote spinal cord repair. J. Biol. 5, 7.

DeVivo, M.J. (1997). Causes and costs of spinal cord injury in the United States. Spinal Cord 35, 809–813.

Edgar, R.E., Best, L.G., Quail, P.A., and Obert, A.D. (1993). Computer-assisted DREZ microcoagulation: posttraumatic spinal deafferentation pain. J. Spinal Disord. 6, 48–56.

Falci, S., Best, L., Bayles, R., Lammertse, D., and Starnes, C. (2002). Dorsal root entry zone microcoagulation for spinal cord injury-related central pain: operative intramedullary electrophysiological guidance and clinical outcome. J. Neurosurg. 97, 193–200.

Gorman, A.L., Yu, C.G., Ruenes, G.R., Daniels, L., and Yezierski, R.P. (2001). Conditions affecting the onset, severity, and progression of a spontaneous pain-like behavior after excitotoxic spinal cord injury. J. Pain 2, 229–240.

Gwak, Y.S., and Hulsebosch, C.E. (2009). Remote astrocytic and microglial activation modulates neuronal hyperexcitability and below-level neuropathic pain after spinal injury in rat. Neuroscience 161, 895–903.

Gwak, Y.S., Hains, B.C., Johnson, K.M., and Hulsebosch, C.E. (2004). Effect of age at time of spinal cord injury on behavioral outcomes in rat. J. Neurotrauma 21, 983–993.

Hains, B.C., Johnson, K.M., Eaton, M.J., Willis, W.D., and Hulsebosch, C.E. (2003). Serotonergic neural precursor cell grafts attenuate bilateral hyperexcitability of dorsal horn neurons after spinal hemisection in rat. Neuroscience 116, 1097–1110.

Hargreaves, K., Dubner, R., Brown, F., Flores, C., and Joris, J. (1988). A new and sensitive method for measuring thermal nociception in cutaneous hyperalgesia. Pain 32, 77–88.

Harvey, L.O. (1986). Efficient estimation of sensory thresholds. Behav. Res. Methods Inst. Comp. 18, 623–632.

Huang, D., and Yu, B. (2010). The mirror-image pain: an unclered phenomenon and its possible mechanism. Neurosci. Biobehav. Rev. 34, 528–532.

Hulsebosch, C.E., Xu, G.Y., Perez-Polo, J.R., Westlund, K.N., Taylor, C.P., and McAdoo, D.J. (2000). Rodent model of chronic central pain after spinal cord contusion injury and effects of gabapentin. J. Neurotrauma 17, 1205–1217.

Jones, T.L., and Sorkin, L.S. (2004). Calcium-permeable alpha-amino-3-hydroxy-5-methyl-4-isoxazolepropionic acid/kainate receptors mediate development, but not maintenance, of secondary allodynia evoked by first-degree burn in the rat. J. Pharmacol. Exp. Ther. 310, 223–229.

Lampert, A., Hains, B.C., and Waxman, S.G. (2006). Upregulation of persistent and ramp sodium current in dorsal horn neurons after spinal cord injury. Exp. Brain. Res. 174, 660–666.

McEwen, M.L., and Springer, J.E. (2006). Quantification of locomotor recovery following spinal cord contusion in adult rats. J. Neurotrauma 23, 1632–1653.

McQuay, H., Carroll, D., Jadad, A.R., Wiffen, P., and Moore, A. (1995). Anticonvulsant drugs for management of pain: a systematic review. BMJ 311, 1047–1052.

McQuay, H.J., Tramer, M., Nye, B.A., Carroll, D., Wiffen, P.J., and Moore, R.A. (1996). A systematic review of antidepressants in neuropathic pain. Pain 68, 217–227.

Milligan, E.D., Mehmert, K.K., Hinde, J.L., Harvey, L.O., Martin, D., Tracey, K.J., Maier, S.F., Watkins, L.R. (2000). Thermal hyperalgesia and mechanical allodynia produced by intrathecal administration of the human immunodeficiency virus-1 (HIV-1) envelope glycoprotein, gp120. Brain Res. 861, 105–116.

Milligan, E.D., O'Connor, K.A., Nguyen, K.T., Armstrong, C.B., Twining, C., Gaykema, R.P., Holguin, A., Martin, D., Maier, S.F., and Watkins, L.R. (2001). Intrathecal HIV-1 envelope glycoprotein gp120 induces enhanced pain states mediated by spinal cord proinflammatory cytokines. J. Neurosci. 21, 2808–2819.

Milligan, E.D., Twining, C., Chacur, M., Biedenkapp, J., O'Connor, K., Poole, S., Tracey, K., Martin, D., Maier, S.F., and Watkins, L.R. (2003). Spinal glia and proinflammatory cytokines mediate mirror-image neuropathic pain in rats. J. Neurosci. 23, 1026–1040.

Ovelmen-Levitt, J., Johnson, B., Bedenbaugh, P., and Nashold, B.S., Jr. (1984). Dorsal root rhizotomy and avulsion in the cat: a comparison of long term effects on dorsal horn neuronal activity. Neurosurgery 15, 921–927.

Penas, C., Casas, C., Robert, I., Fores, J., and Navarro, X. (2009). Cytoskeletal and activity-related changes in spinal motoneurons after root avulsion. J. Neurotrauma 26, 763–779.

Rodrigues Hell, R.C., Silva Costa, M.M., Goes, A.M., and Oliveira, A.L. (2009). Local injection of BDNF producing mesenchymal stem cells increases neuronal survival and synaptic stability following ventral root avulsion. Neurobiol. Dis. 33, 290–300.

Scorisa, J.M., Zanon, R.G., Freria, C.M., and de Oliveira, A.L. (2009). Glatiramer acetate positively influences spinal motoneuron survival and synaptic plasticity after ventral root avulsion. Neurosci. Lett. 451, 34–39.

Siddall, P.J., and Finnerup, N.B. (2006). Pain following spinal cord injury, in: Handbook of Clinical Neurology. F. Cervero and T.S. Jensen (eds), Elsevier: Philadelphia, pps. 689–703.

Siddall, P.J. (2009). Management of neuropathic pain following spinal cord injury: now and in the future. Spinal Cord 47, 352–359.

Siddall, P.J., McClelland, J.M., Rutkowski, S.B., and Cousins, M.J. (2003). A longitudinal study of the prevalence and characteristics of pain in the first 5 years following spinal cord injury. Pain 103, 249–257.

Sorkin, L.S., Yu, A.L., Junger, H., and Doom, C.M. (2002). Antibody directed against GD(2) produces mechanical allodynia, but not thermal hyperalgesia when administered systemically or intrathecally despite its dependence on capsaicin sensitive afferents. Brain Res. 930, 67–74.

Spataro, L.E., Sloane, E.M., Milligan, E.D., Wieseler-Frank, J., Schoeniger, D., Jekich, B.M., Barrientos, R.M., Maier, S.F., and Watkins, L.R. (2004). Spinal gap junctions: potential involvement in pain facilitation. J. Pain 5, 392–405.

Su, H., Zhang, W., Guo, J., Guo, A., Yuan, Q., and Wu, W. (2009). Lithium enhances the neuronal differentiation of neural progenitor cells in vitro and after transplantation into the avulsed ventral horn of adult rats through the secretion of brain-derived neurotrophic factor. J. Neurochem. 108, 1385–1398.

Takahashi, Y., and Nakajima, Y. (1996). Dermatomes in the rat limbs as determined by antidromic stimulation of sensory C-fibers in spinal nerves. Pain 67, 197–202.

Tan, A.M., Stamboulian, S., Chang, Y.W., Zhao, P., Hains, A.B., Waxman, S.G., and Hains, B.C. (2008). Neuropathic pain memory is maintained by Rac1-regulated dendritic spine remodeling after spinal cord injury. J. Neurosci. 28, 13173–13183.

Thompson, S.W., Dray, A., and Urban, L. (1996). Leukemia inhibitory factor induces mechanical allodynia but not thermal hyperalgesia in the juvenile rat. Neuroscience 71, 1091–1094.

Vierck, C.J., Jr., Siddall, P., and Yezierski, R.P. (2000). Pain following spinal cord injury: animal models and mechanistic studies. Pain 89, 1–5.

Yezierski, R.P. (2006). Chapter 21, Pain following spinal cord injury: central mechanisms. Handb. Clin. Neurol. 81, 293-V.

Yezierski, R.P., Liu, S., Ruenes, G.L., Kajander, K.J., and Brewer, K.L. (1998). Excitotoxic spinal cord injury: behavioral and morphological characteristics of a central pain model. Pain 75, 141–155.

Zhao, P., Waxman, S.G., and Hains, B.C. (2007). Extracellular signal-regulated kinase-regulated microglia-neuron signaling by prostaglandin E_2 contributes to pain after spinal cord injury. J. Neurosci. 27, 2357–2368.

Zhou, L.H., Han, S., Xie, Y.Y., Wang, L.L., and Yao, Z.B. (2008). Differences in c-jun and nNOS expression levels in motoneurons following different kinds of axonal injury in adult rats. Brain Cell Biol. 36, 213–227.

Address correspondence to:
Julie Wieseler, Ph.D.
Department of Psychology and Neuroscience
& the Center for Neurosciences
Campus Box 345
University of Colorado at Boulder
Boulder, CO 80309-0345

E-mail: wieseler@colorado.edu